

International Council for  
the Exploration of the Sea

ICES C.M. 1993/L:64  
Theme Session 0

## SPATIAL VARIABILITY OF PHYTOPLANKTON COMMUNITIES IN THE UPWELLING REGION OFF PORTUGAL



Maria Teresa Moita  
Instituto Nacional Investigação das Pescas  
Av. Brasília, 1400 LISBOA, PORTUGAL

### ABSTRACT

The composition and distribution of phytoplankton was studied during a cruise carried out off the coast of Portugal in August 1985. The structure of phytoplankton communities was related to the observed hydrographic conditions and to some geographic features of the area.

The distribution and abundance pattern of total phytoplankton and diatoms, mostly represented by chain-forming species, reflected the direct area of influence of the newly upwelled coastal waters. Small species of dinoflagellates and coccolithophores appeared to be adapted to warmer and more saline offshore waters of the western coast. Coccolithophorids have been related to the northward decreasing influence of the subtropical branch of ENACW, being very abundant at the upwelling center of cape S. Vicente. Different assemblages were associated with different stages of upwelling development during sampling or different patterns of the upwelling process along the coast. Those assemblages were mainly composed by dinoflagellates observed north of cape Roca, e.g. toxic species, and coccolithophores observed in the south.

## 1. INTRODUCTION

The Iberian upwelling system is considered the northern limit of the general upwelling associated with the North Atlantic anticyclonic gyre (Wooster *et al*, 1976). As part of this system, coastal upwelling off portuguese cost occurs seasonally from Spring to early Autumn reaching its maximum intensity in July, August and September (Fiúza *et al*, 1982). Along the western shelf coastal upwelling occurs under cycles of fairly strong and steady northerly winds - the "Portuguese trades", while at the south coast upwelling only takes place when temporary westerly winds occur.

According to Fiúza (1983), the upwelling of the portuguese coast comprises different patterns determined by coastal morphology, the continental shelf/upper slope bathymetry and local winds. In the wide and flat shelf north of the Nazaré canyon the upwelling is fairly homogeneous alongshore although recent studies

to be non negligible (Jorge da Silva, 1992a). South of that region the influence of Lisbon and Setúbal canyons in association with large embayments induces a three dimensionality on the system. South of cape Sines the pattern of the upwelled waters is more regular, thermal gradients are compressed nearshore due to a steep shelf and virtually no shelf break. Waters that upwelled off the southern part of the west coast may turn counterclockwise around cape S.Vicente and merge with waters upwelled locally flowing then eastward along the Algarve shelf break.

Off the portuguese coast the upper 500 m are occupied by two water masses, with different hydrological properties, corresponding to different branches of the Eastern North Atlantic Central Water - ENACW (Fiúza, 1984, Rios, Pérez and Fraga, 1992): the lower (Subpolar) branch, formed W of Biscay Bay is usually found below shelf edge level while the upper (Subtropical) branch of warmer and more saline waters, which is formed south of Azores, is mainly observed off the shelf edge.

The termohaline characteristics of the source of upwelling waters (from 60 to 120m depth) presents a zonal variation as a consequence of the progressive northward decreasing influence of the ENACW subtropical branch. The shelf is occupied by Central Water modified by processes associated with continental margin like upwelling and river runoff (Fiúza, 1984). During spring and summer the whole shelf North of Nazaré tend to be occupied by a nearsurface lens of less saline water resulting from water running southward from Biscay Bay, mixed with modified upwelled water and river plumes (Jorge da Silva, 1992b). An additional salinity front can also be established nearshore due to freshwater runoff.

Some mesoscale structures of phytoplankton pigment concentration, based on Nimbus 7 CZCS images of the portuguese area, have been associated with the dynamics of coastal upwelling (Sousa and Bricaud, 1992). North of Lisbon, filaments and plumes of high pigment concentrations coincide with topographic features such as submarine ridges and can extend zonally 200 km off the west coast. To the south the plumes were observed south of capes along the west coast or parallel to the meridional coast. The relationship between SST and pigment concentration depend upon the stage of the local upwelling event (Sousa and Bricaud, 1992).

Practically no information is available relating the mesoscale variability of phytoplankton communities and the oceanographic variability of the neighboring inshore, and offshore portuguese coastal waters. However, research on the different diatom assemblages in surface sediments has been developed by Abrantes (1988) as an indication of the average upwelling structure of the area. This author relates the pronounced differences observed in the abundance and species dominance between the areas north and south of Nazaré canyon to a higher nutrient availability in the north, either due to a more intense or persistent upwelling or to an additional nutrient input by river discharge.

North of Portugal, the northwestern Iberian coast is characterized by the presence of several flooded tectonic valleys, the Rias Baixas. Several studies were developed inside the Rias or on the neighboring coastal and open sea areas

describing the seasonal cycle of phytoplankton, the spacial distribution of phytoplankton related to some patterns of circulation and distribution of water masses as well as the influence of coastal upwelling on phytoplankton production and succession of species (Margalef et al, 1955; Durán et al, 1956; Varela, 1982; Estrada, 1985; Figueiras and Niell, 1987; Varela et al, 1987a,b.).

The aim of this paper is to describe the mesoscale geographic distribution and composition of phytoplankton observed during CICLOS I cruise carried out off the portuguese coast during the upwelling season and to relate the observed heterogeneities to the hydrographic conditions.

## 2. MATERIAL AND METHODS

As part of a more extended program "Plankton Production Cycles" along the portuguese coast, during the cruise "CICLOS I", carried out by R/V "Noruega", 105 stations were occupied from 21 August to 2 September 1985 covering the entire coast of Portugal. The stations were made along sixteen sections extending from 5 to 80 Km offshore approximately perpendicular to the isobath curves (Fig.1).

Nansen bottles equipped with reversing thermometers were used at depths of 0, 5, 10, 20, 30, 40, 50, 75, 100, 125 and 150m (or near bottom in shallow areas) to collect water samples for salinity, oxygen, nutrients, chlorophyll determination and to phytoplankton identification and counting analysis.

Wind data from a meteorological station located at cape Carvoeiro (Fig.1) were extracted from *Boletim Meteorológico Diário* (INMG, Lisbon). The mean of 4 measures per day was calculated.

Salinity was determined by using a salinometer BECKMAN Mod.RS7-C. Chlorophyll *a* and phaeopigments were determined using a fluorometer Perkin-Elmer Mod.204-A.

Phytoplankton samples were preserved with hexamethylenetetramine buffered formalin to a final concentration of 2% (Thronsdon, 1978). Due to the great number of samples to count savings in time and effort have been achieved by studying one integrated sample per station representing the whole water column (water samples from each depth have been mixed in proportion to the extent of water column they represented). Sometimes it was necessary to study some details of the water column. In those cases samples from each depth were reanalyzed since all the samples were retained for future use. Subsamples of 100 ml were allowed to settle for 3 days. Cells were identified and counted by the Utermohl technique (Hasle, 1978a,b) using a Zeiss IM35 inverted microscope with phase contrast and brightfield illumination as needed. A magnification of 160x was used to enumerate the larger cells in alternate transects of the whole bottom chamber. Very abundant species were counted in one or more crossed-diameter transects up to a number of 200. Smaller forms like flagellates, small dinoflagellates or coccolithophorids, were enumerated in several areas of the chamber (corresponding to 1 ml of settled sample), with a 400x magnification. Cells were identified to species when possible but some could be assigned only to genus or grouped into



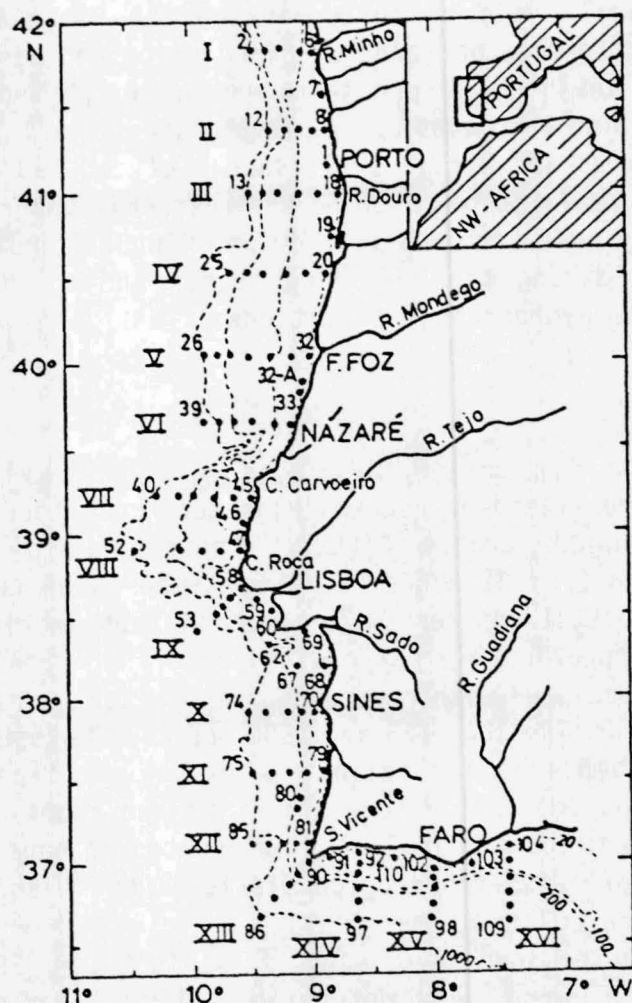


Fig.1. Bathymetry and location of sampling stations during "CICLOS I" cruise. 21 August - 2 September 1985. Automatic weather station was located at C.Carvoeiro.

entities appropriate to taxonomic work (Margalef, 1978). A total of 350 species or taxonomic entities of algae have been identified in the samples observed.

Due to the amount of collected data, a principal component analysis (PCA) was used to synthesize the information and to describe the variability within the phytoplankton data. Because a larger number of zero-abundance values in the data may distort the analysis (Legendre and Legendre, 1979; Blasco *et al*, 1980) only widely distributed organisms (63 taxonomic groups) were included. The criterion of selection includes the species present in more than 15% of the samples. The species used in the analysis are listed in Table 1. PCA was performed using the NTSYS (Numerical Taxonomy and Multivariate System Analysis) software package. The calculations were based on the correlation matrix of transformed counts ( $X = \ln(C+1)$ ) where  $C = \text{cells l}^{-1}$  of selected taxa. The scores of the components were mapped and contours freely traced to show the general patterns.

### 3. RESULTS

#### 3.1. Hydrography

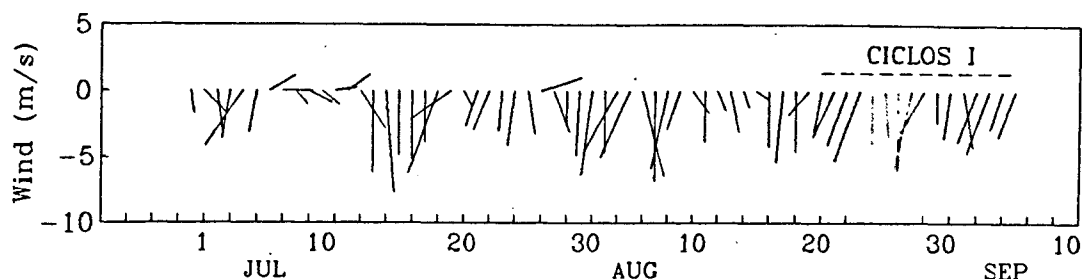


Fig.2. Vector plots of winds at cape Carvoeiro. Sticks point toward the direction the wind was flowing and the length of the stick indicates its magnitude (scale on left axis). The cruise period is indicated.

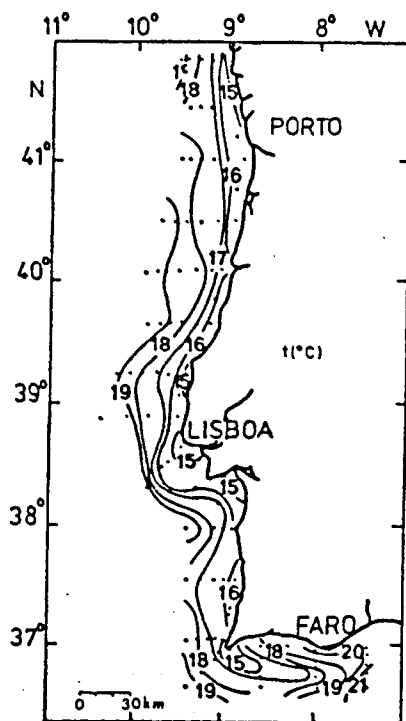


Fig.3. Sea surface temperature ( $^{\circ}\text{C}$ ) during "CICLOS I" cruise.

The winds observed at the meteorological station of cape Carvoeiro ( $39^{\circ}20'N$ ) were weak and variable in the beginning of July (Fig. 2). From 14 July on the wind was persistent from the north (upwelling favorable) although weak to moderate. In August, prior and during the cruise the wind stayed predominantly southward (upwelling favorable) with alternating periods of more or less intensity. During the cruise the wind reached  $7 \text{ m s}^{-1}$  on days 26 and 27 decreasing afterwards.

The pattern of sea surface temperature distribution observed during the cruise (Fig.3) reflected the ongoing conditions of coastal upwelling: isotherms were parallel to coastline being the coldest waters of  $15^{\circ}\text{C}$  and  $16^{\circ}\text{C}$  observed nearshore or south of capes; at the southwestern coast, waters at the upwelling center of cape S.Vicente have turned counterclockwise around the cape flowing eastward along the southern shelf break. Off the west coast temperatures up to  $19^{\circ}\text{C}$  have been observed offshore while at the southern coast  $21^{\circ}\text{C}$  were reached at mouth of Guadiana river.

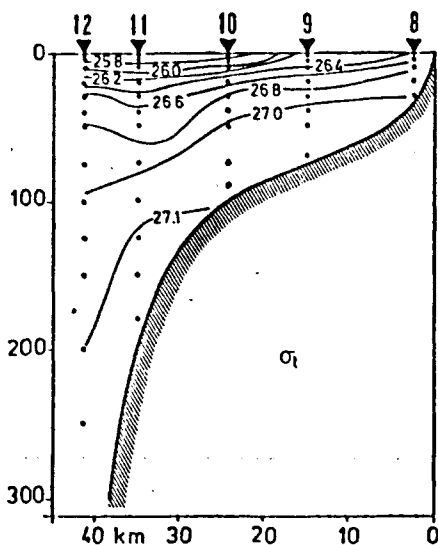
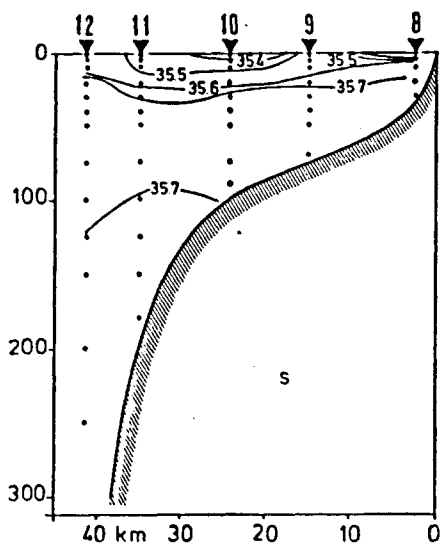
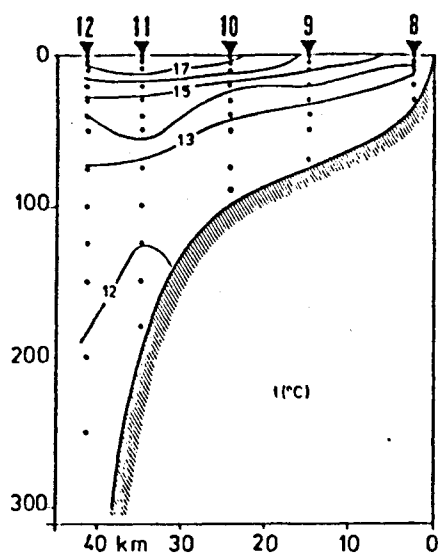


Fig.4. Vertical distribution of temperature ( $^{\circ}\text{C}$ ), salinity and density at section II (north of Oporto) during "CICLOS I" cruise. 22 August.

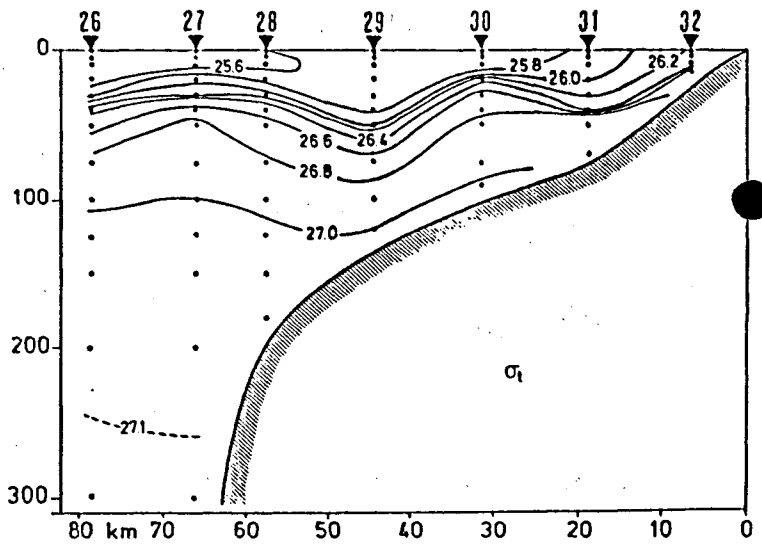
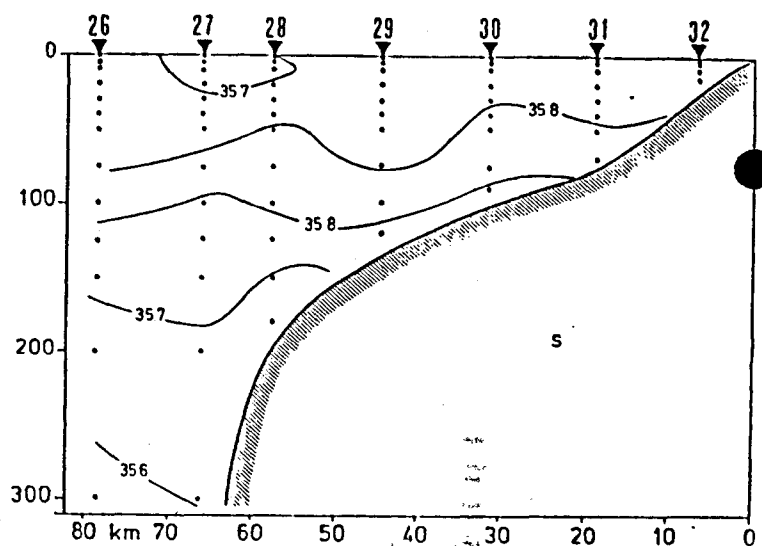
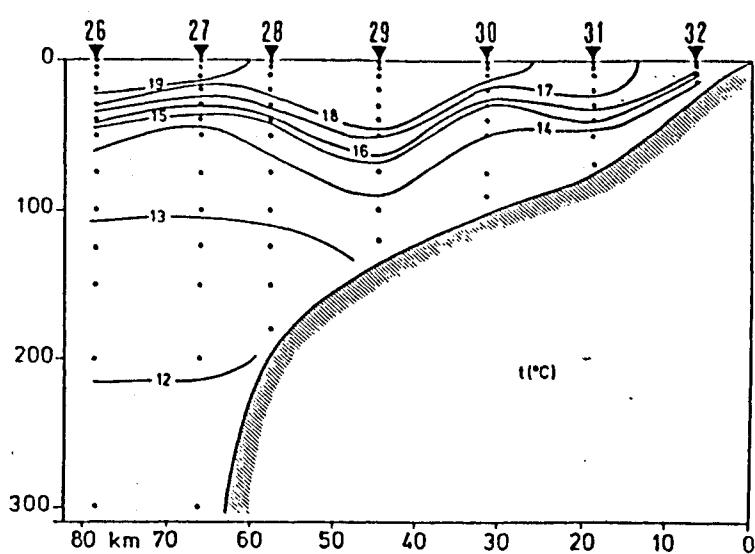


Fig.5. Vertical distribution of temperature ( $^{\circ}\text{C}$ ), salinity and density at section V (F.Foz) during "CICLOS I" cruise. 23-24 August.

Although the pattern of SST distribution (Fig.3) represents the observations taken along the 13 days of cruise, AVHRR images from NOAA-9 satellite (images not shown, processed by the University of Lisbon) confirmed that those features (and consequently coastal upwelling) were apparently maintained during the whole cruise. At sections situated north of Oporto, however (Fig.4), vertical distribution of isopycnals showed that inshore waters were somewhat stratified in a clear indication that the ocean did not respond to the weak winds blowing before and in the beginning of the cruise. To the south of section IV, the ocean

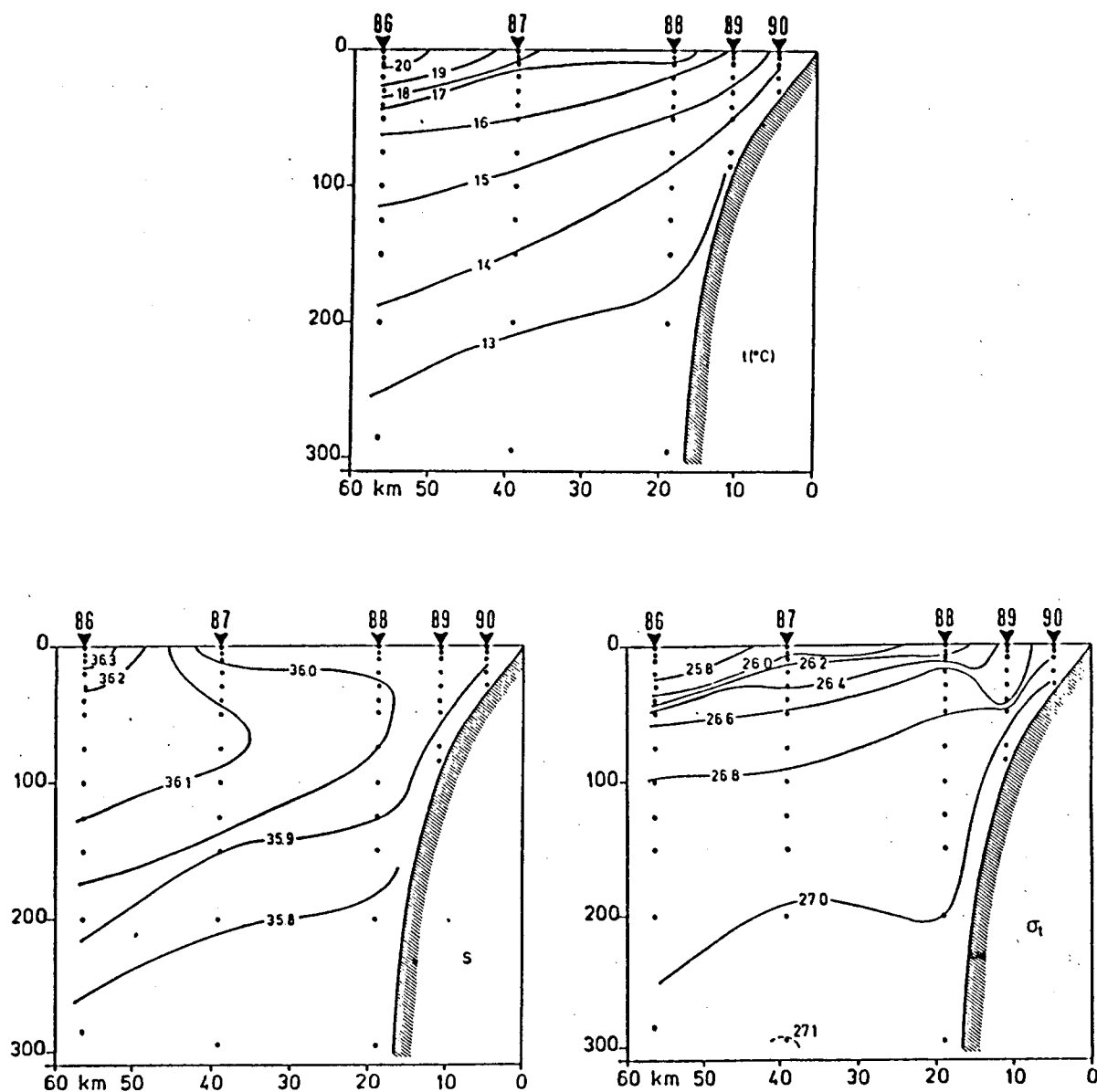


Fig.6. Vertical distribution of temperature ( $^{\circ}\text{C}$ ), salinity and density at section XIII (cape S.Vicente) during "CICLOS I" cruise. 29 August.

was responding to the wind forcing. This was revealed not only by an offshore displacement of isotherms near surface (e.g. section V, Fig.5) but also by a satellite image from 26 August (not shown). Off the southwestern coast, at cape S.Vicente upwelling center (section XIII, Fig.6), there was a remarkable upward of waters from 150-200m that reached the surface levels at the inner station.

The thermohaline characteristics from the offshore station of each section (located over the slope) is shown in Fig.7. The subtropical and the subpolar branches definition lines of ENACW are represented. Waters from surface to approximately 110m depth showed a clear south to north decrease of their salinity values. This was particularly evident south of Tagus and Sado valleys and can be related to a progressive northward decreasing influence of the ENACW subtropical branch. Waters below that depth align through the definition lines represented.

In an attempt to identify the influence of water masses present over the portuguese shelf vertical distributions of temperature, salinity and density at three different sections are also shown (Figs.4, 5 and 6). After Fiúza (1984) it is possible to characterize the subtropical branch of ENACW with values of  $\sigma_t < 27.0$  and the subpolar branch as  $27.1 < \sigma_t < 27.3$ . The upper 300m of sections XIII (Fig.6) and 200 m of section V (Fig.5) were, then, occupied by the subtropical

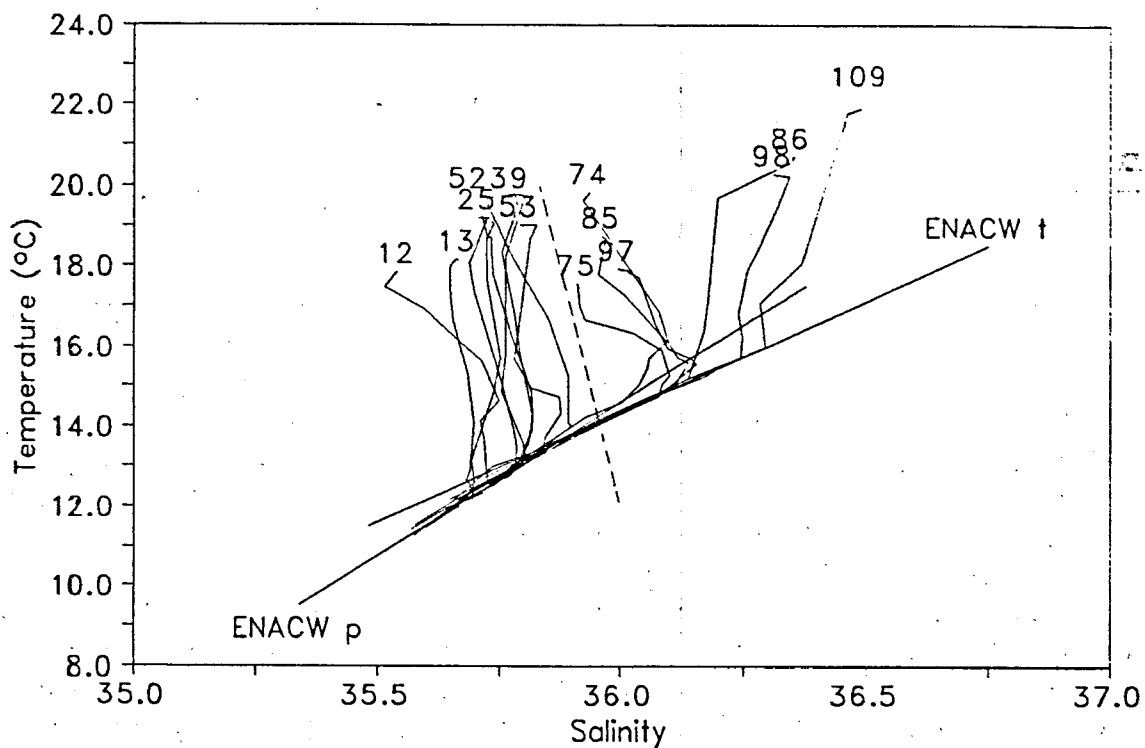


Fig.7. "CICLOS I". T/S diagram of the offshore station of each section. ENACWp - subpolar branch of ENACW; ENACWt - subtropical branch of ENACW. Dashed line: position of Sado and Tagus valleys.



branch of ENACW also characterized by a subsurface salinity maximum. At section II (Fig.4), this branch is still recognizable between 35.7 isohalines while the subpolar branch, with densities higher than 27.1, is observable immediately below 120m being a possible source water for upwelling under stronger winds. At sections V (Fig.5) and XIII (Fig.6) the subpolar branch can only be noticeable below 250m and 300m, respectively.

According to Jorge da Silva (1992b) the isohaline of 35.7 separates at surface the subtropical branch from a nearsurface lens of less saline water which can occupy the whole northern shelf north of the Nazaré canyon. The first 30m of section II seem to be occupied by that lens (Fig.4) which is still visible at the outer-shelf surface waters of section V (fig.6). Fig.8 illustrate the distribution of this lens at surface.

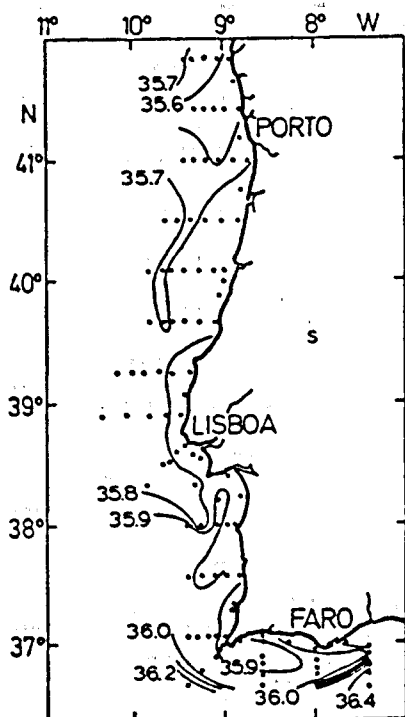


Fig.8. Distribution of salinity at 0m during "CICLOS I" cruise.

### 3.2 - Phytoplankton

The distribution pattern of phytoplankton, expressed by both the biomass (chlorophyll a) at surface or the mean abundance of cells in the water column (Fig.9), followed the pattern of sea surface temperature and therefore were closely related to the upwelling process. Higher biomasses and population densities, reaching values of  $5.5 \text{ mg m}^{-3}$  and  $650 \times 10^3 \text{ cells l}^{-1}$  respectively, were associated with lower temperatures observed inshore, along the western coast or around cape S.Vicente (Fig.2). North of cape Roca phytoplankton-rich waters were extending only 10 to 30 Km offshore and the isolines closely contoured the profile of the continental shelf. At

section IX (Lisbon) the maximum phytoplankton biomass was coinciding with waters upwelling at midshelf. Just like the temperature, the phytoplankton-rich plume turned around the cape S.Vicente and extended eastward over the shelfbreak of southern coast. A band of lower number of cells was observable north of Lisbon coinciding with the shelf-edge (Fig.9).

The distribution of diatoms (Fig.10) was similar to those of chlorophyll and total phytoplankton (Fig.9). Being the major group in higher biomass areas, in agreement with the pattern of surface temperature, it was directly associated with recent upwelled waters. Dinoflagellate populations (Figs.10) were abundant nearshore in the northwestern coast but scarce at the southern coast. At the southwestern coast this group was outlying the upwelling center of cape

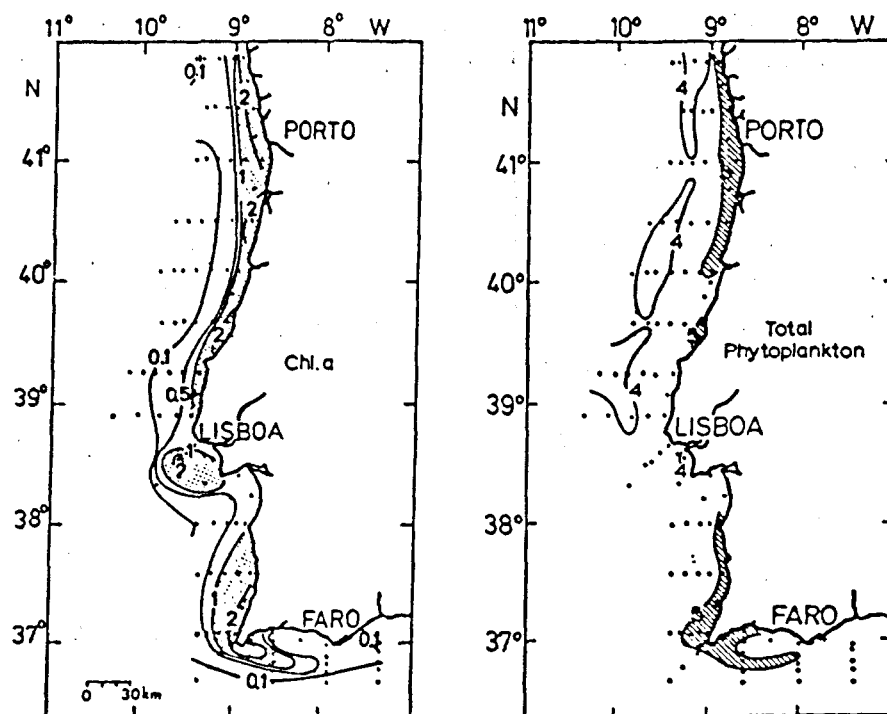


Fig.9. "CICLOS I" cruise. Geographic distribution of chlorophyll a ( $\text{mg m}^{-3}$ ) (left) and total phytoplankton ( $\log \text{no. cells l}^{-1}$ ) (right), averaged in the water column (0-150m).

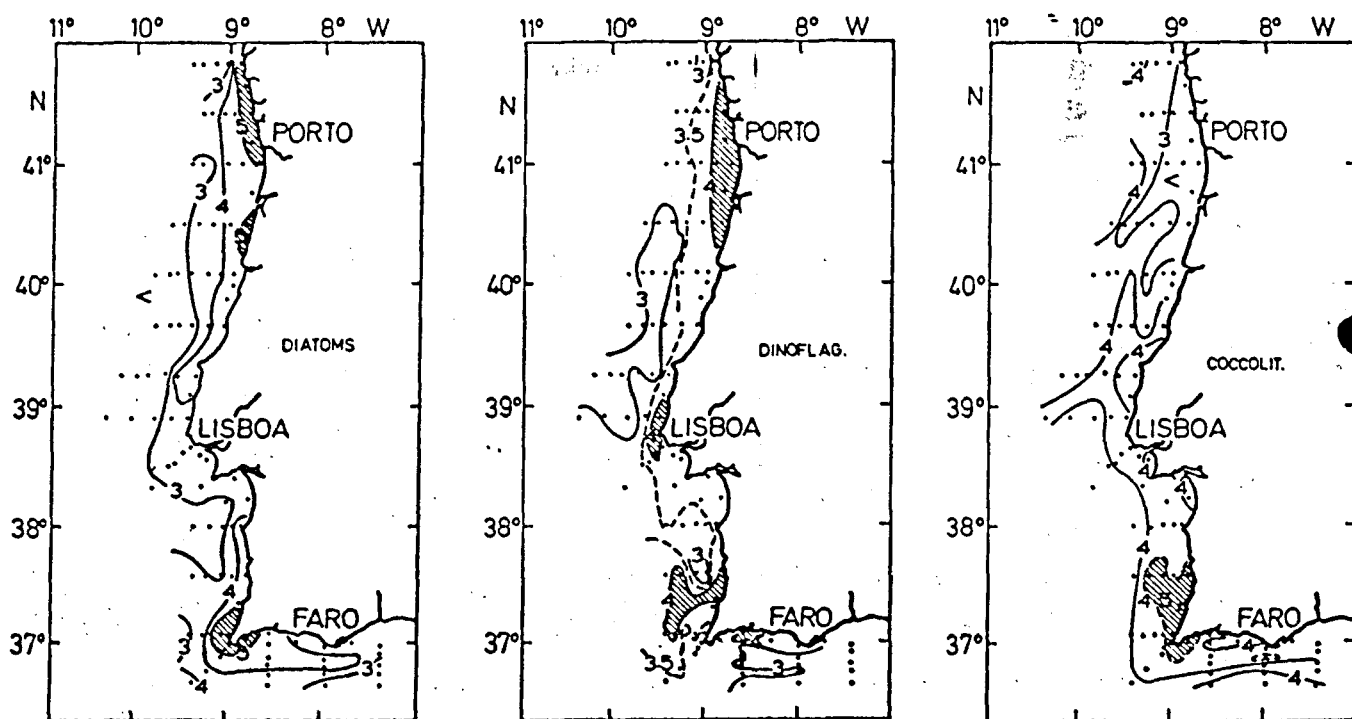


Fig.10. "CICLOS I" cruise. Geographic distribution of phytoplankton groups ( $\log \text{no. cells l}^{-1}$ ) averaged in the water column (0-150m). Left: diatoms. Center: dinoflagellates. Right: coccolithophorids.

S.Vicente. Apparently, newly upwelled waters removed the dinoflagellates from the area of cape where, in turn, coccolithophorids reached their maxima (Figs.10). To the north of Lisbon this group was mainly distributed at mid and outershelf, with the lowest numbers observed at innershelf stations north of F.Foz.

### 3.3 - Principal component analysis and distribution of phytoplankton assemblages

Much information can be gained by studying the distribution of species assemblages rather than individual species, to select groups of species with similar ecological responses. The principal component analysis (PCA) carried out with the 63 taxonomic groups present in at least 15% of the samples showed that the percentage of total variance explained by the first three components was relatively high if it is compared with results obtained by other authors and if it is considered the sampling design used. The first three components explained respectively 26.1%, 13.7% and 4.5% accounting for 44.3% of total variance within the data. The correlation coefficient list of species ordained by their correlation coefficient with PC1 is presented in Table I.

The distribution of the first principal component (Fig.11) is coinciding with the SST and phytoplankton biomass distributions (both chlorophyll or cell abundance) and most of the species had a positive correlation with it as is often the case in such analysis (Estrada and Blasco, 1985). The distribution pattern of PC1 scores seem to separate populations of both small and large diatoms

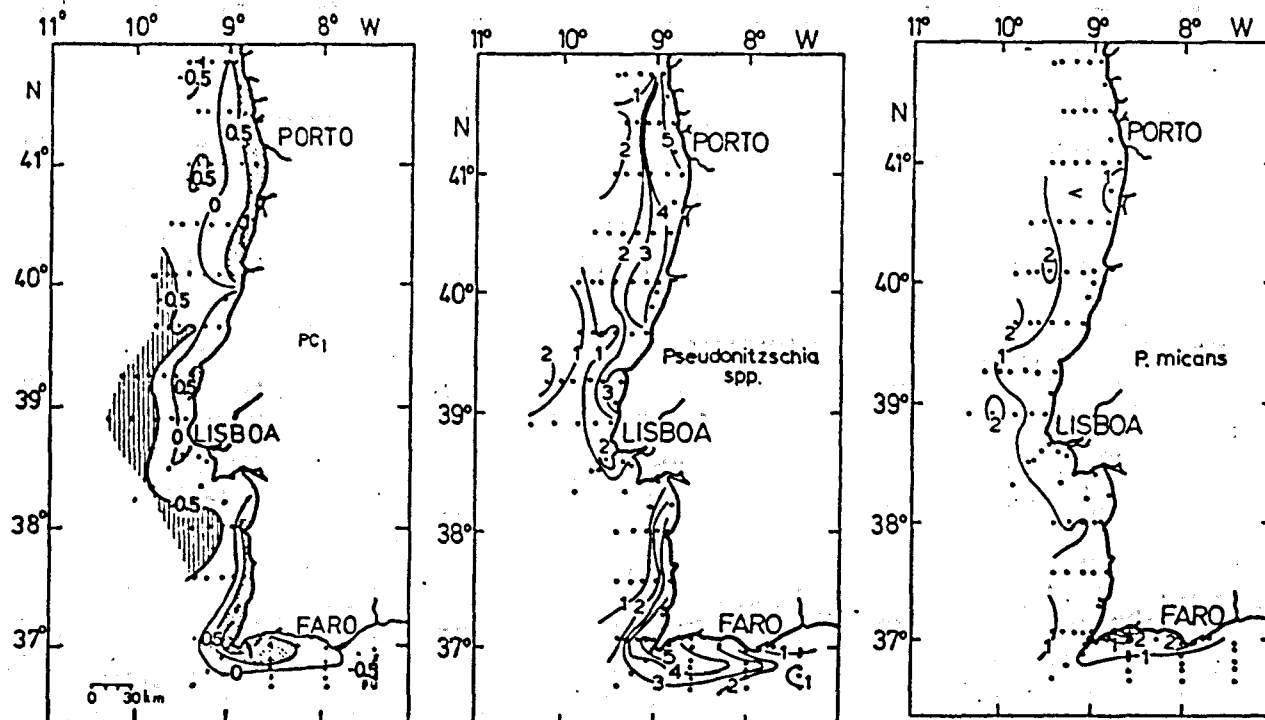


Fig.11: Distribution of PC1 based on the scores computed for each sample (left). Negative areas dotted, positive areas hatched. Distribution of *Pseudonitzschia* spp. and *Prorocentrum micans* (log (no.cells l<sup>-1</sup>) + 1) of opposite loadings in relation to PC1.

Table I. Correlation coefficients of the phytoplankton species and groups selected for principal component analysis with the first three components. Taxon are ordered according to their correlation coefficient with PC1.

Taxon	Components		
	PC1	PC2	PC3
<i>Pseudonitzschia</i> spp.	0.859	0.220	-0.054
<i>Chaetoceros</i> spp.	0.853	0.197	-0.005
<i>Thalassiosira</i> spp.	0.827	-0.114	0.154
<i>Eucampia zodiacus</i> Ehrenberg	0.815	0.205	0.020
<i>Leptocylindrus danicus</i> Cleve	0.802	-0.047	-0.106
<i>Rhizosolenia stolterfothii</i> H.Peragallo	0.797	-0.054	0.019
<i>Navicula</i> spp.	0.791	-0.315	-0.145
<i>Cylindrotheca closterium</i> (Ehrenb.) Reimann & Lewin	0.772	0.058	-0.146
<i>Lauderia annulata</i> Cleve	0.757	-0.143	-0.000
<i>Detonula pumila</i> (Castr.) Shutt	0.715	-0.222	-0.165
<i>Chaetoceros didymum</i> Ehrenberg	0.700	-0.371	-0.160
<i>Protoperidinium</i> spp.	0.696	0.047	0.003
<i>Rhizosolenia</i> spp.	0.683	-0.297	-0.036
<i>Rhizosolenia alata</i> f.alata Brightwell	0.676	0.462	-0.166
undetermined centric diatoms	0.674	0.102	-0.031
<i>Odontella mobiliensis</i> (Bailey) Round	0.658	0.103	0.295
<i>Thalassiothrix</i> spp.	0.653	-0.314	-0.281
<i>Cerataulina pelagica</i> (Cleve) Hendey	0.649	0.378	0.143
<i>Protoperidinium bipes</i> (Paulsen) Balech	0.643	-0.256	0.023
<i>Thalassiosira anguste-lineata</i> (A.Schmi.) Fryxel and Hasle	0.641	-0.258	-0.321
<i>Hemiaulus sinensis</i> Grevillard	0.626	-0.598	-0.068
<i>Protoperidinium diabolium</i> (Cleve) Balech	0.610	-0.203	-0.191
<i>Thalassionema nitzschioides</i> Grunow	0.604	0.348	0.132
<i>Ceratium furca</i> (Ehrenb.) Clap. and Lachm.	0.553	0.471	-0.002
<i>Distephanus speculum</i> Ehrenberg	0.537	-0.357	-0.129
<i>Thalassiosira rotula</i> Meunier	0.527	-0.364	-0.027
<i>Scrippsiella trochoidea</i> (Stein) Loeblich	0.525	0.267	0.352
<i>Cocconeis</i> spp.	0.507	-0.392	-0.123
<i>Diploneis</i> spp.	0.504	-0.048	0.172
<i>Dinophysis acuta</i> Ehrenberg	0.504	0.494	0.052
undetermined euglenophyceans	0.494	-0.082	0.432
<i>Dinophysis</i> spp.	0.465	0.508	-0.140
<i>Protoperidinium divergens</i> (Ehrenb.) Balech	0.449	-0.040	-0.265
<i>Amphora</i> spp.	0.422	-0.449	0.124
<i>Ceratium fusus</i> (Ehrenb.) Dujardin	0.415	0.747	-0.036
undetermined pennate diatoms	0.383	-0.408	-0.054
undetermined dinoflagellates	0.378	0.260	0.486
<i>Noctiluca scintillans</i> (Macartney) Ehrenberg	0.378	0.376	0.149
<i>Coccolithus pelagicus</i> (Wallich) Schiller	0.372	-0.438	0.440
<i>Gephyrocapsa oceanica</i> Kamptner	0.369	-0.486	-0.054
<i>Asteromphalus fiabellatus</i> (de Bréb.) Greville	0.350	-0.123	-0.142
<i>Protoperidinium depressum</i> (Bail.) Balech	0.319	0.521	0.209
<i>Paralia sulcata</i> (Ehrenb.) Cleve	0.317	0.179	0.454
<i>Ceratium massiliense</i> (Gourr.) Jorgensen	0.263	0.744	0.142
<i>Syracosphaera pulchra</i> Lohmann	0.262	-0.470	-0.064
<i>Dinophysis tripos</i> Gourret	0.237	0.571	-0.061
<i>Ceratium</i> spp.	0.233	0.595	-0.170

Table I (cont.)

Taxon	Components		
	PC1	PC2	PC3
<u>Leptocylindrus mediterraneus</u> (Perag.) Hasle	0.181	0.412	-0.128
<u>Pronoctiluca spinifera</u> (Lohmann) Schiller	0.143	0.259	-0.144
<u>Thalassiosira eccentrica</u> (Ehrenb.) Cleve	0.137	-0.025	0.231
<u>Protoperidinium globulum</u> (Stein) Balech	0.121	-0.327	0.460
undetermined coccolithophorids	0.119	-0.675	-0.063
<u>Prorocentrum triestinum</u> Schiller	0.119	-0.336	0.296
<u>Nitzschia</u> spp.	0.104	0.153	-0.086
<u>Helicosphaera carteri</u> (Wallich) Kamptner	0.082	-0.567	0.180
<u>Coronosphaera mediterranea</u> (Lohmann) Kamptner	0.036	-0.514	0.439
<u>Gonyaulax</u> spp.	0.026	-0.141	-0.229
<u>Amphidoma caudata</u> Halldall	0.017	-0.076	0.215
<u>Braarudosphaera bigelowii</u> (Gran & Braarud) Deflandre	-0.014	0.109	0.101
<u>Dictyocha fibula</u> Ehrenberg	-0.023	-0.518	-0.154
<u>Emiliania huxleyi</u> (Lohmann) Hay and Mohler	-0.126	-0.689	0.079
<u>Thoracosphaera heimii</u> (Lohmann) Kamptner	-0.244	-0.274	0.442
<u>Prorocentrum micans</u> Ehrenberg	-0.249	-0.048	-0.299

present in inshore waters like *Pseudonitzschia* spp., *Chaetoceros* spp., *Thalassiosira* spp., *Eucampia zoodiacus*, *Leptocylindrus danicus*, *Rhizosolenia stolterfothii* and *Navicula* spp., from several species of other groups occurring at offshore stratified warmer and more saline waters (*Prorocentrum micans*, *Thoracosphaera heimii*, *Emiliania huxleyi*). Species with higher positive and negative correlation coefficients with the first component were *Pseudonitzschia* spp. (mainly composed by *Pseudonitzschia pungens* f. *pungens*, *Pseudonitzschia fraudulenta* and probably *P. cuspidata* (Hasle, personal communication)) and *Prorocentrum micans*, respectively (Fig.11). *P. micans* although associated with PC1 and offshore waters along the whole west coast was detached from PC1 at southern coast where inshore conditions were also favorable to its growth.

The scores of the second principal component had a north-south distribution. Either higher positive or negative values were observed inshore respectively to the north of Nazaré canyon and to the south of cape Sines, in this case associated with the upwelling center of cape S.Vicente (Fig.12). PC2 was defined by *Ceratium fusus* (Fig.12) and other *Ceratium* species like *C. massiliense* and several other species like *Protoperidinium depressum* or toxic dinoflagellate from genus *Dinophysis*. The distributions of *D.acuta* and *D.tripos* have already been described (Moita, 1993). The dinoflagellates were separated by the component from a community of diatoms like *Hemiaulus sinensis* (Fig.12) and



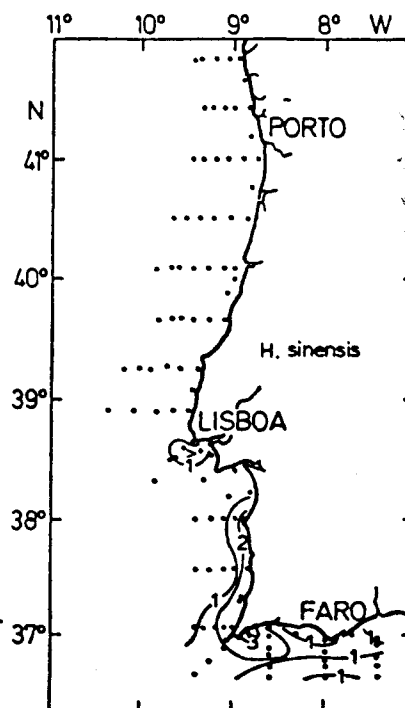
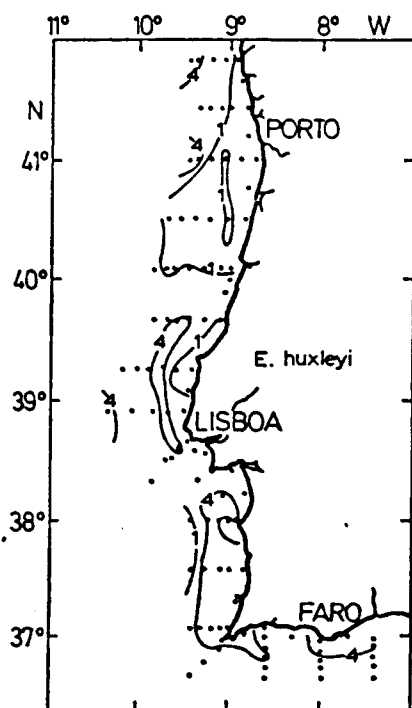
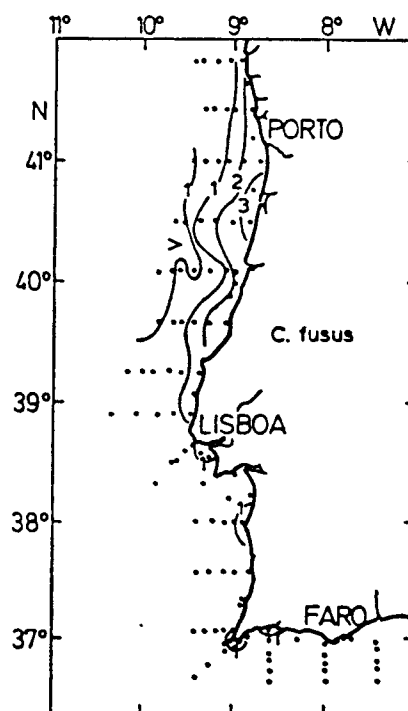
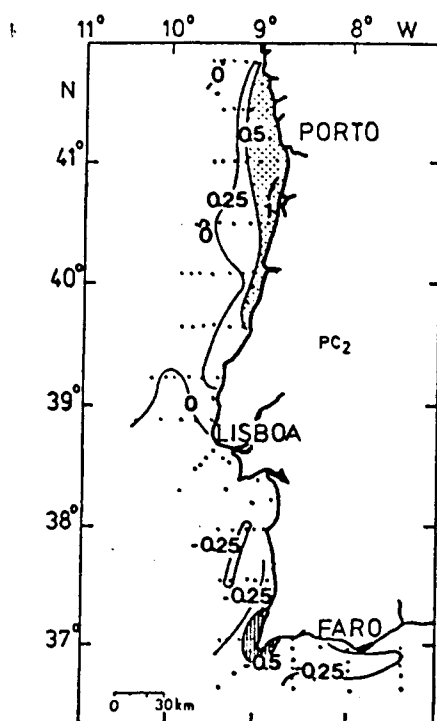


Fig.12. Distribution of PC2 and of *Ceratium fusus* ( $\log(\text{no. cells l}^{-1}) + 1$ ) positively correlated with the component (above). Distribution of *Emiliana huxleyi* and *Hemiaulus sinensis* ( $\log(\text{no. cells l}^{-1}) + 1$ ) of negative loadings in relation to PC2 (below).

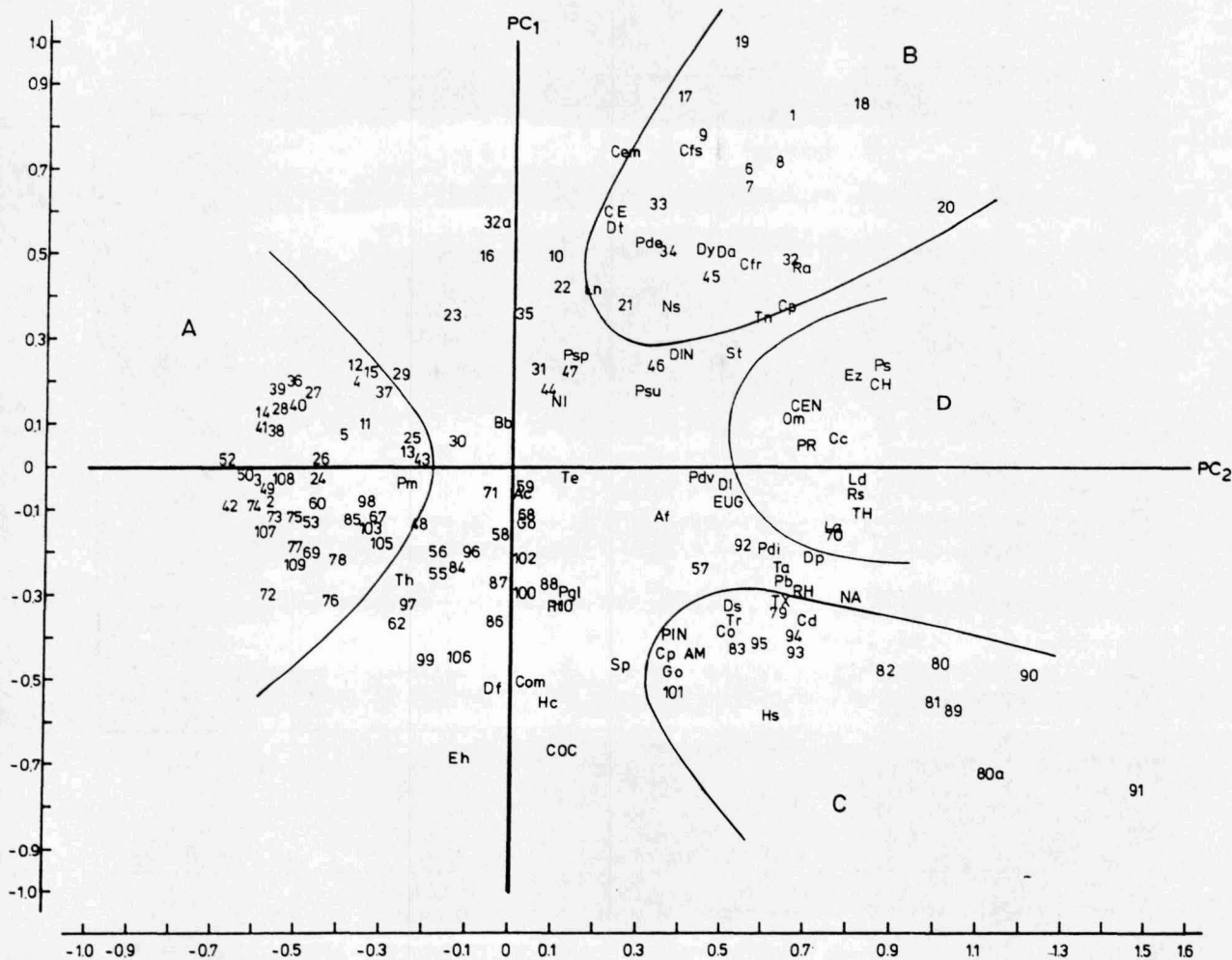


Fig. 13. Position of most frequent taxonomic groups (vectors) and the projection of stations in the space defined by PC1 and PC2. A, B, C, D: Phytoplankton assemblages defined by PC1 and PC2. Abbreviations: PS - *Pseudonitzschia* spp., CH - *Chaetoceros* spp., TH - *Thalassiosira* spp., Ez - *Eucampia zoodiacus*, Ld - *Leptocylindrus danicus*, Rs - *Rhizosolenia stolterfothii*, NA - *Navicula* spp., Cc - *Cylindrotheca closterium*, La - *Lauderia annulata*, Dp - *Detonula pumila*, Cd - *Chaetoceros didymum*, PR - *Protoperidinium* spp., RH - *Rhizosolenia* spp., Ra - *Rhizosolenia alata*, CEN - undetermined centric diatoms, Om - *Odontella mobiliensis*, TX - *Thalassiothrix* spp., Cp - *Cerataulina pelagica*, Pb - *Protoperidinium bipes*, Ta - *Thalassiosira anguste-lineata*, Hs - *Hemiaulus sinensis*, Pdi - *Protoperidinium diabolum*, Tn - *Thalassionema nitzschioides*, Cfr - *Ceratium furca*, Ds - *Distephanus speculum*, Tr - *Thalassiosira rotula*, St - *Scrippsiella trochoidea*, CO - *Cocconeis* spp., DI - *Diploneis* spp., Da - *Dinophysis acuta*, EUG - undetermined euglenophyceans, DY - *Dinophysis* spp., Pdv - *Protoperidinium divergens*, AM - *Amphora* spp., Cfs - *Ceratium fusus*, PIN - undetermined pennate diatoms, DIN - undetermined dinoflagellates, Ns - *Noctiluca scintillans*, Cp - *Coccolithus pelagicus*, Go - *Gephyrocapsa oceanica*, Af - *Asteromphalus flabellatus*, Pde - *Protoperidinium depressum*, Psu - *Paralia sulcata*, Cem - *Ceratium massiliense*, Sp - *Syracosphaera pulchra*, Dt - *Dinophysis tripos*, CE - *Ceratium* spp., Lm - *Leptocylindrus mediterraneus*, Psp - *Pronoctiluca spinifera*, Te - *Thalassiosira eccentrica*, Pgl - *Protoperidinium globulum*, COC - undetermined coccolithophorids, Pt - *Prorocentrum triestinum*, NI - *Nitzschia* spp., Hc - *Helicosphaera carteri*, Com - *Coronosphaera mediterranea*, GO - *Gonyaulax* spp., Ac - *Amphidoma caudata*, Bb - *Braarudosphaera bigelowii*, Df - *Dictyochea fibula*, Eh - *Emiliania huxleyi*, Th - *Thoracosphaera heimii*, Pm - *Prorocentrum micans*.

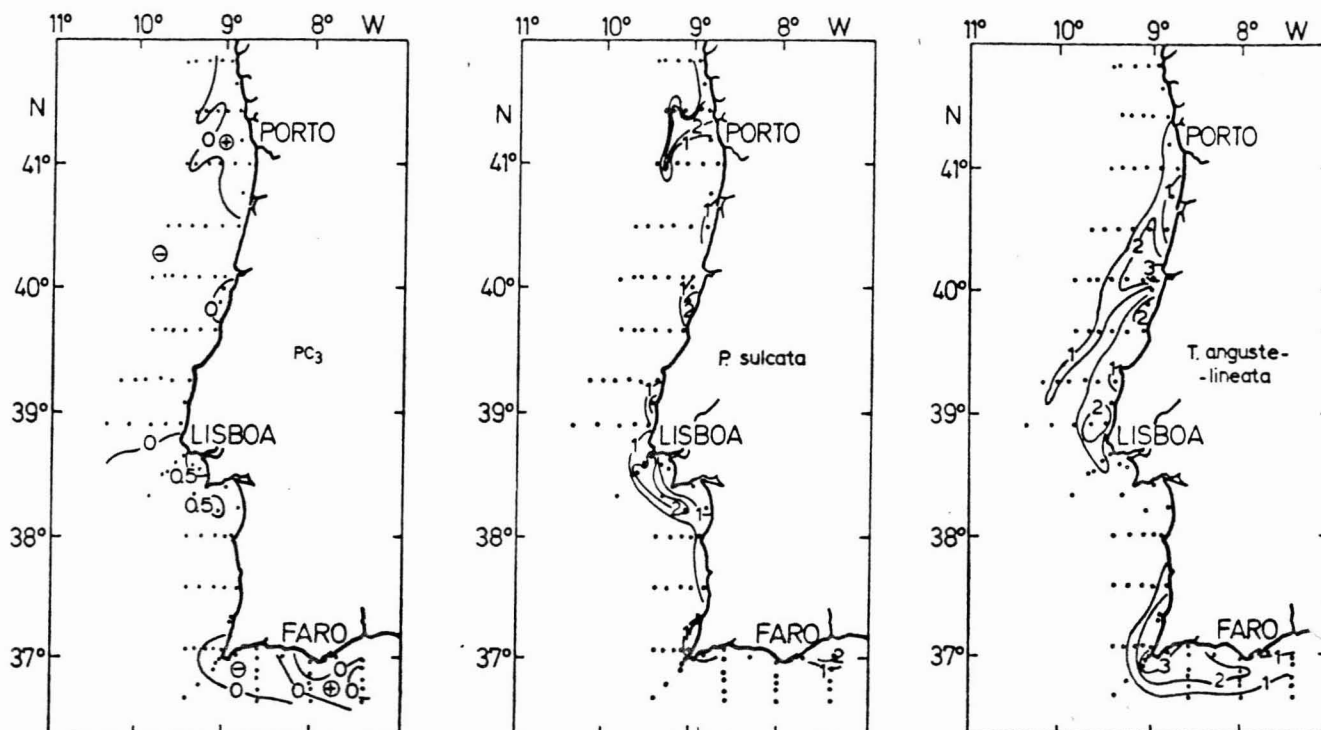


Fig. 14. Distribution of PC3 based on the scores computed for each sample (left). Distribution of *Paralia sulcata* and *Thalassiosira anguste-lineata* (log (no. cells  $l^{-1}$ ) + 1) of opposite loadings in relation to PC1.

pennate diatoms as *Amphora* spp. and *Cocconeis* spp. mixed with coccolithophorids such as *Emiliana huxleyi* (Fig.12), *Helicosphaera carteri*, *Coronosphaera mediterranea*, *Syracosphaera pulchra*, *Gephyrocapsa oceanica*. This component is likely to reflect not only different characteristics of waters in the north or in the south but also different phases of upwelling development.

Fig.13 shows the different assemblages as generated by the first two components of the principal component analysis as well as the projection of stations in the space of the components.

Neither the distribution of the scores of the third principal component nor the ordination of the species with respect to the component gave much insight into the significance of PC3 (Fig.14). Positive scores were observed in the three first sections in opposition to negative values at cape S.Vicente. This seems to suggest this component expressed differences in the conditions of stratification observed during the cruise (Figs.5 and 7), partly already explained by PC1 and PC2. However, PC3 did not present a north-south or a cross-shore distribution as PC2 and PC1. Higher positive values were observed in the area of Lisbon. *Paralia sulcata*, considered as an upwelling related species in the portuguese coast

(Abrantes, 1988) was distributed like inshore patches along the coast (Fig.13). This species had positive loadings with the component together with dinoflagellates and coccolithophorids as *Coccolithus pelagicus*, *Coronosphaera mediterranea*. Conversely, the group negatively correlated with the component included *Thalassiosira anguste-lineata*, *P.micans* and other diatoms and dinoflagellates. A possible explanation to the difficulties observed in the interpretation of PC3 variability was likely to the occurrence of the Guttman or horseshoe effect (Flos et al, 1986) during multivariate analysis. According to these authors if the variables (species) are not independent and the first dimensions are strongly dominant, that seems to be the case, it is quite sure that the third dimension is a combination of the two previous ones and quite impossible to explain.

Table II. Phytoplankton assemblages defined by the projection of the species in the space of PC1 and PC2.

Group A	Group B	Group C1
-----	-----	-----
<i>Prorocentrum micans</i>	<i>Ceratium fusus</i>	<i>Amphora</i> spp.
<i>Thoracosphaera heimii</i>	<i>Ceratium massiliense</i>	<i>Cocconeis</i> spp.
<i>Emiliana huxleyi</i>	<i>Ceratium</i> spp.	pennate diatoms
	<i>Protoperidinium depressum</i>	
Group D	<i>Dinophysis tripos</i>	Group C2
-----	<i>Dinophysis</i> spp.	-----
<i>Pseudonitzschia</i> spp.	<i>Dinophysis acuta</i>	<i>Emiliana huxleyi</i>
<i>Chaetoceros</i> spp.	<i>Ceratium furca</i>	<i>Hemiaulus sinensis</i>
<i>Thalassiosira</i> spp.	<i>Rhizosolenia alata</i>	<i>Helicosphaera carterae</i>
<i>Eucampia zoodiacus</i>		<i>Coronosphaera mediterranea</i>
<i>Leptocylindrus danicus</i>		<i>Gephyrocapsa oceanica</i>
<i>Rhizosolenia stolterfothii</i>		<i>Syracosphaera pulchra</i>

#### 4. DISCUSSION AND CONCLUSIONS

During CICLOS I, the first of a series of cruises to study the plankton production cycles off the portuguese coast, several trends of phytoplankton distribution appeared to be related to conditions favorable to coastal upwelling. The winds, although upwelling favorable (blowing southward) were weak with some periods of higher intensity such as in the middle of the cruise, on 25 and 26 August (Fig.2). The ocean responded to wind forcing at least after the first three sections. This was confirmed by the distribution of isotherms parallel to the western coast line (Fig.3), pattern also followed by phytoplankton-rich

waters as well as by diatoms (Figs. 9, 10). Additionally, an eastward extension of the waters upwelled on the southwestern coast, rich in phytoplankton, was observed after cape S.Vicente along the shelf break of the southern coast. This filament is a recurrent pattern associated with the upwelling dynamics of the cape (Fiúza, 1983), whose waters contains high pigment concentrations (Sousa and Bricaud, 1992).

There was a band of lower numbers of phytoplankton cells along the outershelf-shelfbreak of the northwestern coast (Fig.9). This feature was temptingly associated with a coinciding band of zooplankton biomass observed during the same cruise (Cunha, 1993), reflecting the effect of predation by zooplankton on algae. Such structure of both phytoplankton and zooplankton communities to coincide would be an indication of a steady interrelation between the two groups (Cushing, 1971) in good agreement with a fairly homogeneous alongshore upwelling described to the northwestern coast (Fiúza, 1983). That band, with lower numbers of phytoplankton, could also result from sinking of phytoplankton at the shelf edge, in a circulation cell established as a consequence of upwelling development (Jorge da Silva, 1992c). At the species level, it is possible to identify a similar feature on *Pseudonitzschia* spp. distribution (Fig.11).

The main source of variability (26.1%) within the data (Fig.11) was explained by species from group D and group A (Fig.13, Table II). Group D, composed by chain-forming diatoms, was associated with the upwelling process (i.e. lower temperatures, Fig.3) and followed the general patterns described to the phytoplankton rich waters. Group A, with a very low diversity of species was associated with stratified offshore waters.

Coccolithophorids (Figure 6), in great part belonging to nannoplankton were dominated by *Emiliania huxleyi* (Fig.12) and formed the assemblage designated by C2 (Table II). The distribution of this group was one of the more interesting during the cruise since it was clearly associated to the area of influence of the subtropical branch of Eastern North Atlantic Central Water (ENACWt). Higher values of *E.huxleyi* were observed at cape S.Vicente where ENACWt upwelled waters reached the surface. The species was coastal in the southwestern coast, north of Lisbon being present at mid shelf and north of F.Foz being observed at the shelf edge waters. This species and coccolithophorids in general were removed from costal waters north of F.Foz. This fact was related both to the presence of a less saline water observed in the area (Fig.8) and to the slight characteristics of ENACWt in that region (Fig.4). It is important to refer that there are scarce references to the occurrence of coccolithophorids in coastal waters of Rías baixas in Galicia that could corroborate our results. Estrada (1984) has associated the presence of *E.huxleyi* in that region with offshore waters although the species could appeared in the proximity of the rías.

A mixture of chain forming diatoms and dinoflagellates was observed in the ria of Vigo and was considered as being typical of the high biomass situations following enrichment events in the rias (Margalef *et al*; 1955, Durán *et al*, 1956). Such an assemblage, the mixture of groups B (positive species with PC2



(Fig.12)) and D (positive species with PC1 (Fig.11)) characterized the region north of F.Foz being the group responsible for higher biomasses observed nearshore. Estrada (1984) has associated a similar mixture with a low salinity water extending offshore from the mouth of the rias. The nearsurface lens of less saline water that results from water running southward from Biscay Bay, mixed with modified upwelled water and river plumes has been observed in the northern shelf off portuguese coast (Jorge da Silva, 1992b) and during the cruise (Fig.8). Group B seem to be related with that water, since most of the species, in particular *Ceratium* species were mainly distributed in the upper 20m. Nevertheless, the abundance of this group in the first sections could also reflect the stratification conditions observed at inshore stations in the beginning of the cruise. Elongated diatoms such as *Pseudonitzschia* and *Rhizosolenia* belonging to group D can also find suitable environment for their development in situations with some physical stability (Sournia, 1982).

The differences observed in groups B distributed at inshore stations in the north (mainly composed by dinoflagellates) and group C (mixture of group C1, diatoms of benthic characteristics and C2, coccolithophorids) at inshore stations in the south, expressed not only the different thermohaline characteristics of waters but also different stages of upwelling development in the two regions. In fact, as observed in cape S.Vicente (Fig.6), upwelling was much more active and the waters from bottom reached the surface. This fact explains the presence of group C1. In the north the waters were more stratified that explains the presence of dinoflagellate communities, e.g. toxic species.

#### ACKNOWLEDGEMENTS

I would like to thank C. Afonso Dias for helpful discussions to prepare this work. Thanks are also due to my colleagues Ana Costa, A. Moraes and G. Vilarinho for their help on the identification and counting of phytoplankton samples and to Maria da Conceição Almeida who prepared the figures. I am grateful to the captain and crew of the R/V "Noruega" by their excellent support at sea. This work was partly funded by Junta Nacional de Investigação Científica e Tecnológica, Project JNICT/MAR/87344.

#### REFERENCES:

- Abrantes, F., 1988. Diatom assemblages as upwelling indicators in surface sediments off Portugal. Marine Geology, 85: 15-39.
- Basco, D., M. Estrada and B. Jones, 1980. Relationship between the phytoplankton distribution and composition and the hydrography in the northwest African upwelling region near Cabo Corbeiro. Deep-Sea Research, 27A: 799-821.
- Cunha, M.E., 1993. Spatial variation of the zooplankton biomass over the portuguese continental shelf. ICES C.M., L:63, 23pp.
- Cushing, D.H., 1971. Upwelling and the production of fish. Adv.mar.Biol., 9: 255-334.
- Durán, M., F. Saiz, M. López-Benito and R. Margalef, 1956. El fitoplancton de la ría de Vigo de abril de 1954 a junio de 1955. Inv.Pesq., 4: 67-95.
- Estrada, M., 1984. Phytoplankton composition off Galicia (Northwest Spain). J.Plank.Res., 6: 417-434.

- Estrada, M. and D. Blasco, 1985. Phytoplankton assemblages in coastal upwelling areas. In: International Symposium of Upwelling of W Africa. C.Bas, R.Margalef and P.Rubias (Ed.). Instituto de Investigaciones Pesqueras, Barcelona, 379-402.
- Figueiras, F.G. and F.X. Niell, 1987. Composición del fitoplancton de la Ría de Pontevedra (NO de España). Inv.Pesq. 51: 371-409.
- Figueiras, F.G. and A.F. Ríos, 1993. Phytoplankton succession, red tides and the hydrographic regime in the Rias Baixas of Galicia. In: Toxic Phytoplankton Blooms in the Sea, T. Smayda and Y. Shimizu (Eds.), Elsevier, Amsterdam, 239-244.
- Fiúza, A., M.E. Macedo and M.R. Guerreiro, 1982. Climatological space and time variation of the Portuguese coastal upwelling. Ocean.Acta, 5: 31-40.
- Fiúza, A., 1983. Upwelling patterns off Portugal. In: Coastal Upwelling, its Sediment Record. Part A. Responses of the Sedimentary Regime to Present Coastal Upwelling, E.Suess and J. Thied (Eds.). Plenum, New York, 85-98.
- Fiúza, A., 1984. Hidrologia e dinâmica das águas costeiras de Portugal. Doctoral thesis, University of Lisbon, 294pp. (in portuguese).
- Flos, J., F.A. Ascioti, J.D. Carroll, S. Dallot, S. Frontier, J.C. Gower, R.L. Haedrich and A. Laurec, 1986. Data analysis in pelagic community studies. In: NATO ASI Series, G14. Developments in Numerical Ecology. P. Legendre et L. Legendre (Eds.), Springer-Verlag, Berlín, 495-520.
- Hasle, G.R., 1978a. The inverted microscope method. In: Monographs on Oceanic Methodology. 6. Phytoplankton Manual. A. Sournia (Ed.). UNESCO, Paris, 88-96.
- Hasle, G.R., 1978b. Using the inverted microscope. In: Monographs on Oceanic Methodology. 6. Phytoplankton Manual. A. Sournia (Ed.). UNESCO, Paris, 191-196.
- Jorge da Silva, A., 1992a. Dependence of upwelling related circulation on wind forcing and stratification over the portuguese northern shelf. ICES C.M., C:17, 12pp.
- Jorge da Silva, A., 1992b. Contribuição do Instituto Hidrográfico para o projecto JNICT 87344 - Resultados do cruzeiro CECIR XII, Maio 1987. REL TF-OF-7/92, Instituto Hidrográfico, Lisbon, 29pp. (unpublished manuscript)(in portuguese).
- Jorge da Silva, A., 1992c. Contribuição do Instituto Hidrográfico para o projecto JNICT 87344 - Resultados do cruzeiro CECIR XIII, Agosto 1987. REL TF-OF-8/92, Instituto Hidrográfico, Lisbon, 43pp. (unpublished manuscript)(in portuguese).
- Legendre, L. et P. Legendre, 1979. Ecologie numérique.I.II. Ed.Masson, Paris, 197 + 254pp.
- Margalef, R., 1978. Phytoplankton communities in upwelling areas. The example of NW Africa. Oecol.Aquat., 3: 97-132.
- Margalef, R., M. Durán and F. Saiz, 1955. El fitoplancton de la ría de Vigo de enero de 1953 a marzo de 1954. Inv.Pesq., 2, 85-129.
- Moita, M.T., 1993. Development of toxic dinoflagellates in relation to the upwelling patterns off Portugal. In: Toxic Phytoplankton Blooms in the Sea, T.Smayda and Y.Shimizu (Eds.), Elsevier, Amsterdam, 299-304.
- Rios, A.F., F.F. Pérez and F. Fraga, 1992. Water masses in the upper and middle North Atlantic Ocean east of the Azores. Deep-Sea Research, 39, 645-658.
- Sournia, A., 1982. Form and function in marine phytoplankton. Biol.Rev., 57: 347-394.
- Sousa, F.M. and A. Bricaud, 1992. Satellite derived phytoplankton pigment structures in the portuguese upwelling area. J.Geophys.Res., 97: 11,343-11,356.
- Thronsen, J., 1978. Preservation and storage. In: Monographs on Oceanic Methodology. 6. Phytoplankton Manual. A.Sournia (Ed.). UNESCO, Paris, 69-74.
- Varela, M., 1982. Composición y distribución del fitoplancton de las rías de Muros, Arosa y plataforma continental próxima en Septiembre de 1978. Bol.Inst. Esp.Ocean., 7: 191-222.
- Varela, M., J.M. Cabanas, M.J. Campos, E. Penas, X. Sánchez, A. Larrañaga, F.F. Castillejo, G.D. Río, 1987a. Composición y distribución del fitoplancton en la plataforma de Galicia durante la campaña "BROGAN-684" (junio de 1984). Bol.Inst.Esp.Ocean., 4: 75-94.
- Varela, M., M.J. Campos, J.M. Cabanas, F.F. Castillejo, G.D. Río, 1987b. Composición y distribución del fitoplancton en la plataforma de Galicia durante la campaña "BROGAN-984" (septiembre-octubre de 1984). Bol.Inst. Esp.Ocean., 4: 95-106.
- Wooster, W., A. Bakun and D. McLain, 1976. The seasonal upwelling cycle along the eastern boundary of the North Atlantic. J.Mar.Res., 34: 131-141.